

## High-Elongation Fiber Mats by Electrospinning of Polyoxymethylene

Jian-Wei Lu, Zhan-Peng Zhang, Xiang-Zhong Ren, Yi-Zhang Chen, Jian Yu, and Zhao-Xia Guo\*

*Institute of Polymer Science and Engineering, Department of Chemical Engineering, School of Materials Science and Engineering, Tsinghua University, Beijing 100084, P. R. China*

Received December 27, 2007

Revised Manuscript Received April 9, 2008

Electrospinning is a recently explored simple and versatile fabrication technique for producing nano- to microscale fibers. The electrospun fiber mats possess a number of characteristics such as high specific surface area, high aspect ratio, and high porosity as a result of random deposition of the fibers, which allow a wide range of potential applications such as optoelectronics, sensor technology, catalysis, filtration, and medicine.<sup>1,2</sup> The mechanical properties of the electrospun fibers or mats are usually different from those of the corresponding bulk materials. Sometimes, the difference is enormous and surprising.<sup>3–5</sup> For example, Gu et al.<sup>4</sup> reported a Young's modulus of 50 GPa for polyacrylonitrile single nanofibers, which is much greater than that of the corresponding cast film (1.2 GPa). Kim et al.<sup>5</sup> observed the phenomenon of "necking" with poly(methyl methacrylate) (PMMA)/montmorillonite nanocomposite electrospun single fibers, whereas PMMA is known as a brittle plastic.

Polyoxymethylene (POM) is a versatile engineering plastic.<sup>6,7</sup> It is widely used in automobile and electronic industries due to good properties such as good strength, stiffness, abrasion, and chemical resistance.<sup>8,9</sup> Although almost 100 polymer solutions or melts have been electrospun into fibers,<sup>4</sup> to the best of our knowledge, electrospinning of POM has not yet been reported due to presumably poor solubility in common solvents. However, POM is soluble in 1,1,1,3,3,3-hexafluoro-2-propanol (HFIP), which is frequently used in electrospinning of natural biopolymers such as collagen and chitin.<sup>10–13</sup> In this work, electrospinning of POM solutions in HFIP is investigated, and to our surprise, a very high elongation to break was observed with the POM electrospun fiber mats.

Figure 1 shows the morphology of the electrospun POM mat obtained from a 5 wt % solution at 30 °C with a relative humidity of 40%. The average diameter is 940 nm, and microporous structure was observed with an average pore size of 150 nm. It is well-known that microporous structure is frequently obtained when volatile solvents are used for electrospinning,<sup>14,15</sup> and that high relative humidity also favors formation of pores.<sup>1,16</sup> HFIP is a volatile solvent with a boiling point of 58 °C. The formation of microporous structure in the current case is understandable, although the electrospun fibers of biopolymers reported so far have no obvious pores.<sup>10–13</sup>

The mechanical properties of the nonwoven POM electrospun mats were measured by tensile tests after thorough drying at 40 °C under vacuum, and a typical load–elongation curve is shown in Figure 2a. Elongation of 460% was observed. For comparison, the elongation at break of bulk POM such as a tensile bar obtained from injection molding is known to be

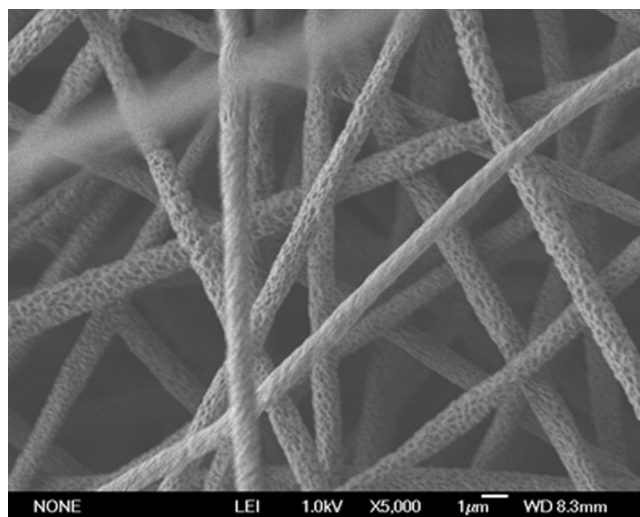


**Figure 1.** FESEM micrograph of the electrospun POM fibers.

40–50%,<sup>9</sup> and that of the thin film cast from the same solution used for electrospinning is only 1%. Therefore, the elongation at break of the electrospun nonwoven mat is about 10-fold of that of the bulk tensile bar and about 460-fold of that of the cast film. Such high elongation seems to be only reported, up to now in the field of electrospinning, for electrospun mats of elastomers<sup>17–19</sup> such as polyurethane (PU), elastomer-containing blends such as PU/poly(vinyl chloride) blend,<sup>20</sup> and core/shell structured fibers obtained from coaxial electrospinning where an elastomer was used as one of the components.<sup>21</sup>

POM is known as a plastic having poor toughness.<sup>7,22</sup> In order to understand the surprising mechanical deformation of the POM electrospun mats, the stretching process during tensile test was carefully observed both macroscopically and microscopically. Macroscopically, the whole specimen is almost homogeneously elongated during tensile test. Only the regions near the two ends (fixing areas) are obviously wider and less stretched (Figure 3). Some plastics such as bulk high-density polyethylene have a very high elongation (e.g., 300–1000%) during tensile tests due to cold drawing,<sup>23</sup> and the phenomenon of necking is observed at the yield point. In this work, necking of the specimen was not observed, indicating that the high elongation observed with the electrospun POM mat does not belong to the phenomenon of traditional cold drawing due to very different morphology.

In order to observe the change in fiber morphology during stretching, tensile tests were stopped at various elongations, and the samples were observed by field emission scanning electron microscopy (FESEM). Necking of single fibers was not observed within the scope of observation. POM is extremely sensible to electron beam, and therefore it is very difficult to observe the fibers closely and carefully. For the same reason, an attempt to observe the stretching of single POM fibers with transmission electron microscopy (TEM) has failed. However, FESEM micrographs presented in Figure 4 show clearly the extent of fiber orientation and fiber diameter change during stretching. At 5% elongation, the fibers are randomly arranged, and there is no change in fiber diameter (940 nm). When the elongation reaches 30%, the fibers are partially oriented along the direction of stretching, and the average fiber diameter has almost no change (930 nm). At 90% elongation, the fibers are almost

\* Corresponding author. E-mail: guozx@mail.tsinghua.edu.cn.

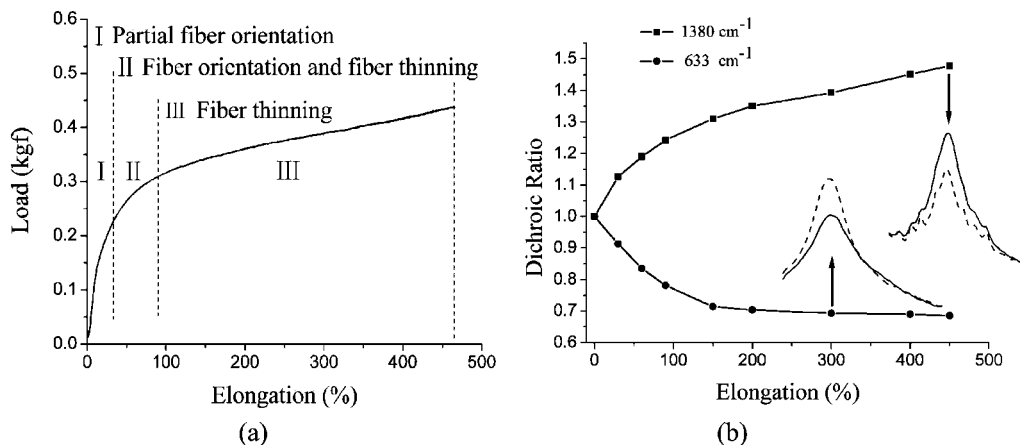


**Figure 2.** (a) Load–elongation curve of the electrospun POM mat: region I (0–30%), region II (30–90%), and region III (90–breakage). (b) In-situ dichroic ratios of the peaks at 1380 and 633 cm<sup>-1</sup> as a function of tensile elongation.

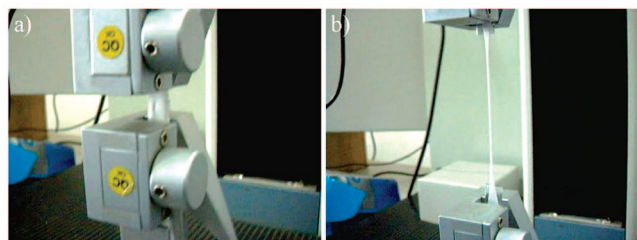


**Figure 3.** Macroscopic view of the stretching process: (a) 0% elongation; (b) 388% elongation.

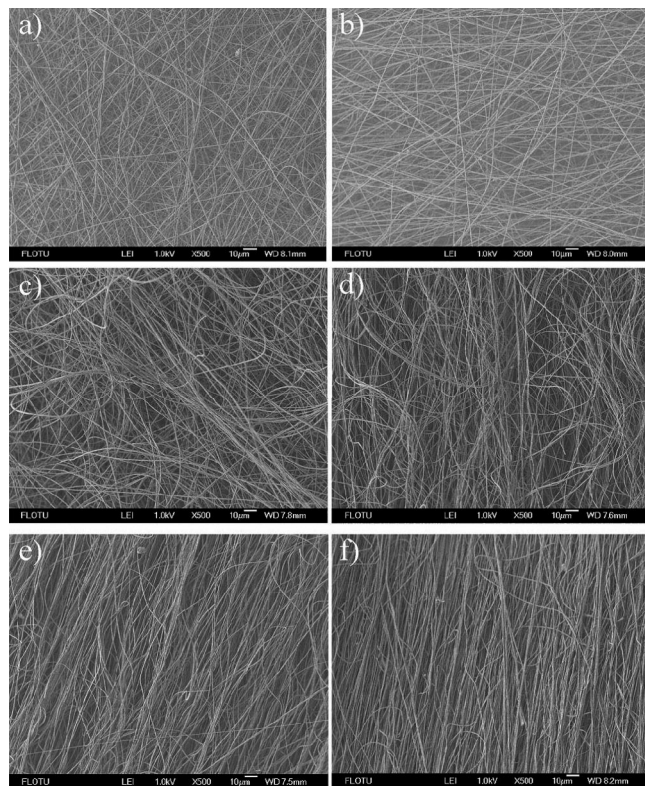


**Figure 4.** FESEM micrographs of the stretched fiber mats at various elongations: (a) 0%, (b) 5%, (c) 30%, (d) 90%, (e) 200%, (f) 388%.

aligned along the direction of stretching and the average fiber diameter decreases to 770 nm. When the sample is further stretched to 200% and 388%, the fibers are well-aligned along the direction of stretching, and the average fiber diameter

decreases further to 540 and 390 nm, respectively. On the basis of this observation, the load–elongation curve can be divided into three regions as shown in Figure 2a. In region I (0–30% elongation), the fibers arrange their positions and do not become thinner during stretching. Elongation increases slowly with the increase of the load. In region III (90–breakage), the fibers are already aligned along the direction of stretching and become increasingly thinner with continuous stretching of the specimen. Elongation increases rapidly with the increase of the load. Region II (30–90% elongation) is the transition region. The easy orientation and stretching of the fibers could be related to the lack of bonding sites among fibers and weak intermolecular interaction due to fast solvent evaporation during electrospinning and lack of inter- and intramolecular hydrogen bonding.

The molecular orientation during stretching was examined by polarized Fourier transform infrared (FTIR)<sup>24,25</sup> and two-dimensional wide-angle X-ray diffraction (2D WAXD).<sup>26</sup> The dichroic ratios for peaks at 1380 [ $\omega(\text{CH}_2)$ ] and 633 cm<sup>-1</sup> [ $\delta(\text{OCO}) + \nu_a(\text{COC})$ ]<sup>27</sup> are shown in Figure 2b. The first peak should show a strong parallel dichroism when the molecular chain axis is oriented along the elongation direction, while the latter should show a strong perpendicular dichroism.<sup>27</sup> As shown in Figure 2b, there is no molecular orientation before stretching due to the random arrangement of the fibers. The degree of molecular orientation increases significantly during the initial stage of stretching (0–150% elongation). Beyond 150% elongation, the degree of molecular orientation only increases slightly when the elongation increases further. According to the 2D WAXD patterns, there is no crystal orientation before stretching, the crystal *c* axis is gradually oriented parallel to the direction of stretching, and obvious crystal orientation is only observed at high strain.

Considering the results of polarized FTIR and 2D WAXD along with those of FESEM, it seems that the molecular orientation in the initial stage of stretching (<150% elongation, mainly regions I and II in Figure 2a) is mainly caused by fiber orientation and stretching of the amorphous molecules which are in rubbery state and more easily stretched than the crystalline molecules. The crystal orientation is only obvious at the later stage of stretching where the fibers are aligned and the stress is high. The easy orientation of POM molecules during stretching may be related to weak inter- and intramolecular interaction. However, it is noted that the degrees of molecular and crystal orientation are much lower than those in the hot rolling POM films<sup>27</sup> and die-drawing POM samples.<sup>28</sup> This could be related to imperfect fiber orientation. As shown in Figure 2a, there are

always some parts of the fibers which are not aligned along the direction of stretching in the stretched electrospun mat, even at high elongation.

The high degree of crystallinity and large crystal size of POM are often to blame for its poor toughness.<sup>29</sup> The degree of crystallinity of the as-spun fibers and those stretched to various elongations were measured by differential scanning calorimetry (DSC) and compared to those of the cast film and virgin POM. The results have shown that the degree of crystallinity<sup>30</sup> of the as-spun fibers is 47.1%, which is 7.5% less than that of the cast film (54.6%) and 13.9% less than that of virgin POM (61.0%). This is in agreement with the trend found in the literature where the degree of crystallinity of the electrospun fibers is usually lower than that of the corresponding cast film or virgin polymer.<sup>31–33</sup> It is noted that the degree of crystallinity is almost unchanged during stretching. The crystal size in the electrospun POM fibers must be very small due to the confinement of the small fiber diameter. The lower degree of crystallinity and smaller crystal size could contribute to the surprisingly high elongation.

In conclusion, POM can be successfully electrospun into fibers using HFIP as the solvent. The POM electrospun mats obtained from 5 wt % solution show a very high elongation which is about 10 times that of the bulk tensile bar. The high elongation of the electrospun mat could be related to fiber and molecular orientation during stretching, lower degree of crystallinity, and smaller crystal size.

**Acknowledgment.** We are grateful to the referees for their helpful suggestions.

**Supporting Information Available:** Details on materials, experiments, and characterization. This material is available free of charge via the Internet at <http://pubs.acs.org>.

## References and Notes

- (1) Greiner, A.; Wendorff, J. H. *Angew. Chem., Int. Ed.* **2007**, *30*, 5670–5703.
- (2) Huang, Z. M.; Zhang, Y. Z.; Kotaki, M.; Ramakrishna, S. *Compos. Sci. Technol.* **2003**, *63*, 2223–2253.
- (3) Arinstein, A.; Burman, M.; Gendelman, O.; Zussman, E. *Nat. Nanotechnol.* **2007**, *2*, 59–62.
- (4) Gu, S. Y.; Wu, Q. L.; Ren, J.; Vancso, G. J. *Macromol. Rapid Commun.* **2005**, *26*, 716–720.
- (5) Kim, G. M.; Lach, R.; Michler, G. H.; Chang, Y. W. *Macromol. Rapid Commun.* **2005**, *26*, 728–733.
- (6) Samon, J. M.; Schultz, J. M.; Hsiao, B. S.; Khot, S.; Johnson, H. R. *Polymer* **2001**, *42*, 1547–1559.
- (7) Gao, X. L.; Qu, C.; Fu, Q. *Polym. Int.* **2004**, *53*, 1666–1671.
- (8) Luftl, S.; Archodoulaki, V. M.; Glantschnig, M.; Seidler, S. *J. Mater. Sci.* **2007**, *42*, 1351–1359.
- (9) Hu, Y. L.; Ye, L. *Polym-Plast. Technol. Eng.* **2006**, *45*, 839–844.
- (10) Park, K. E.; Jung, S. Y.; Lee, S. J.; Min, B. M.; Park, W. H. *Int. J. Biol. Macromol.* **2006**, *38*, 165–173.
- (11) Rho, K. S.; Jeong, L.; Lee, G.; Seo, B. M.; Park, Y. J.; Hong, S. D.; Roh, S.; Cho, J. J.; Park, W. H.; Min, B. M. *Biomaterials* **2006**, *27*, 1452–1461.
- (12) Wnek, G. E.; Carr, M. E.; Simpson, D. G.; Bowlin, G. L. *Nano Lett.* **2003**, *3*, 213–216.
- (13) Kwon, I. K.; Matsuda, T. *Biomacromolecules* **2005**, *6*, 2096–2105.
- (14) Bognitzki, M.; Czado, W.; Frese, T.; Schaper, A.; Hellwig, M.; Steinhart, M.; Greiner, A.; Wendorff, J. H. *Adv. Mater.* **2001**, *13*, 70–72.
- (15) Casper, C. L.; Stephens, J. S.; Tassi, N. G.; Bruce Chase, D.; Rabolt, J. F. *Macromolecules* **2004**, *37*, 573–578.
- (16) Megelski, S.; Stephens, J. S.; Bruce Chase, D.; Rabolt, J. F. *Macromolecules* **2002**, *35*, 8456–8466.
- (17) Pedicini, A.; Farris, R. J. *Polymer* **2003**, *44*, 6857–6862.
- (18) McKee, M. G.; Park, T.; Unal, S.; Yilgor, I.; Long, T. E. *Polymer* **2005**, *46*, 2011–2015.
- (19) Sen, R.; Zhao, B.; Perea, D.; Itkis, M. E.; Hu, H.; Love, J.; Bekyarova, E.; Haddon, R. C. *Nano Lett.* **2004**, *4*, 459–464.
- (20) Lee, K. H.; Kim, H. Y.; Ryu, Y. J.; Kim, K. W.; Choi, S. W. *J. Polym. Sci., Polym. Phys.* **2003**, *41*, 1256–1262.
- (21) Han, X. J.; Huang, Z. M.; He, C. L.; Liu, L. *High Perform. Polym.* **2007**, *19*, 147–159.
- (22) Cheng, Z. G.; Wang, Q. *Polym. Int.* **2006**, *55*, 1075–1080.
- (23) Grulke, E. A. In *Polymer Process Engineering*; PTR Prentice Hall: Upper Saddle River, NJ, 1994; p 418.
- (24) Zhang, X. Q.; Kong, L.; Rottstegge, J.; Xu, D. F.; Wang, D. J. *J. Phys. Chem. B* **2007**, *111*, 11642–11645.
- (25) Bianco, A.; Lardino, G.; Manuelli, A.; Bertarelli, C.; Zerbi, G. *ChemPhysChem* **2007**, *8*, 510–514.
- (26) Liu, Y.; Cui, L.; Guan, F. X.; Gao, Y.; Hedin, N. E.; Zhu, L.; Fong, H. *Macromolecules* **2007**, *40*, 6283–6290.
- (27) Tadokoro, H.; Kobayashi, M.; Kawaguchi, Y.; Kobayashi, A.; Murahashi, S. *J. Chem. Phys.* **1963**, *38*, 703–721.
- (28) Mohanraj, J.; Bonner, M. J.; Barton, D. C.; Ward, I. M. *Polymer* **2006**, *47*, 5897–5908.
- (29) Gao, X. L.; Qu, C.; Zhang, Q.; Peng, Y.; Fu, Q. *Macromol. Mater. Eng.* **2004**, *289*, 41–48.
- (30) Wilski, H. *Makromol. Chem.* **1971**, *150*, 209–222.
- (31) Li, Y.; Huang, Z. M.; Lu, Y. D. *Eur. Polym. J.* **2006**, *42*, 1696–1704.
- (32) Lee, K. H.; Kim, H. Y.; Khil, M. S.; Ra, Y. M.; Lee, D. R. *Polymer* **2003**, *44*, 1287–1294.
- (33) Dersch, R.; Liu, T. Q.; Schaper, A. K.; Greiner, A.; Wendorff, J. H. *J. Polym. Sci., Polym. Chem.* **2003**, *41*, 545–553.

MA702881K